Solar photocatalytic degradation of methyl orange using PbS-ZnS/electrospun fiber composites

IOP Conf. Series: Materials Science and Engineering **556** (2019) 012035 doi:10.1088/1757-899X/556/1/012035

Solar photocatalytic degradation of methyl orange using PbS-ZnS/electrospun fiber composites

Jie Yang, Haiqun Chen, Haifei Chen*
School of Petroleum Engineering, Changzhou University, Changzhou, Jiangsu, China
E-mail: chfs@cczu.edu.cn

Abstract. A facile, efficient approach to fabricate PbS-ZnS heterojunction/electrospun fiber composites with micro-nano-sized structure was reported, involving the preparing of electrospun fibers by high-voltage electrospun technology and the synthesizing of chalcogenide semiconductors by low temperature hydrothermal method. The PbS-ZnS/electrospun fiber composites exhibited high photocatalytic activity for the degradation of methyl orange under ultraviolet (UV) light irradiation of solar light. Compared with titanium dioxide and the PbS-ZnS powder, PbS-ZnS/electrospun fiber composites exhibited excellent reusability with high photocatalytic efficiencies, indicative of its suitability for the solar photocatalytic applications. The residual mass of photodegradation of methyl orange in 300 min was 1.23%.

Keywords: Solar photocatalytic; Electrostatic spinning; Degradation; PbS-ZnS/electrospun fiber composites

1. Introduction

Since the discovery of photocatalytic degradation pollutants in water using TiO_2 by Fujishima in the year of 1972[1], photocatalytic degradation pollutants had been considered as one of the most promising avenue solar energy conversion methods. However, pure semiconducting photocatalyst powders are facing the challenge of large-scale application due to their low degradation rate because of the fast recombination of photo-generated electron/hole pairs and the aggregation of semiconducting particles[2, 3]. Therefore, semiconducting photocatalyst powders had been widely grafted onto organic [4-6] or inorganic carriers [7-9]. It was proved that the carriers could improve the photocatalytic activity as well as the stability of semiconducting phtocatalysts[10].

Inorganic carriers still have some shortcomings such as poor flexibility, low light transmittance, difficulty of loading and processing, etc[11]. Polymers have good flexibility, good film forming properties, high light transmittance and are easy to process compared with Inorganic carriers[12]. Therefore, the use of polymer as a photocatalyst carrier has become a hot topic of current research[13]. Fluorocarbon polymers have good photodegradation resistance, chemical resistance, heat resistance and dielectric properties. It is a good photocatalyst carrier that has attracted more and more attention. Studies have shown that composite materials have good degradation resistance and repeatability [6, 12] .

In this paper, PbS-ZnS/electrospun fiber composites were prepared by supporting PbS-ZnS heterojunction on the FVDF/SMA polymer fibers in the way of hydrothermal synthesis. The photocatalytic performance of the composites was studied by the mercury lamp which simulating ultraviolet (UV) light irradiation of solar light.

2. Experimental

2.1. Materials

Polyvinylidene Fluoride (PVDF) was supplied from Shanghai 3F New Material Co., Styrene-maleic anhydride (SMA) was purchased from Shanghai SpecTek petrochemical high tech Co., Ltd. N, N-dimethylacetamide(DMAC) was purchased from Shanghai Pilot Chemical Co., Ltd. Thiourea, lead nitrate and zinc nitrate were obtained from Sinopharm Shanghai Chemical Reagent Co., Ltd, acetone was brought from Shanghai Su Yi Chemical Reagent Co., Ltd. All chemicals were used as received.

2.2. Electrospinning of PVDF/SMA polymer fiber

A typical electrospinning process prepared the PVDF/SMA polymer fiber. 0.41g SMA and 3.6g PVDF were added into the mixture of acetone and DMAC in a stirred three-necked flask with N2 protection. Afier stirring 24 hours, the solution was electrospun at 24 KV positive voltage, 16 cm working distance, and flow 1.2 ml per hour. All process steps were operated at room temperature. The mat was cut to 5.0cm×5.0cm in dimension for the follow-up experiments.

2.3. Preparation of PbS-ZnS/electrospun fiber composite

The as-prepared electrospun fibers were put into 25 ml, 0.25 mol/L zinc nitrate for 12 h to form the complex between the fiber and the Zn^{2+}. Then the fibers were removed from the solution, washed with distilled water for three times, and dried in a vacuum for 2 h at 60 ℃. Subsequently, the fibers were put into a 50 mL sealed Teflon-lined stainless steel autoclave, which include desired concentration of thiourea solution. The autoclave was placed in an oven for 12 h at 120℃, and then it was cooled to room temperature. The ZnS/electrospun fiber composites were washed with distilled water under ultrasonic vibrations in order to remove the byproducts and unreacted precursor, and were dried in vacuum for 3 h at 60 ℃.

The dried fibers were immersed in 25ml, 0.25 mol/L lead nitrate aqueous solution at room temperature for 24h. Then the fibers were removed from the solution, washed with distilled water for three times, and dried in a vacuum for 2 h at 60 ℃. Subsequently, the fibers were put into a 50 mL sealed Teflon-lined stainless steel autoclave, which include desired concentration of thiourea solution. After being cooled, washed and dried, the PbS-ZnS/electrospun fiber composites were prepared.

As a comparative experiment, the PbS-ZnS powders were prepared by the similar conditions, while the latter was not loaded on the electrospun fiber mats.

2.4. Phtocatalytic reaction

Photocatalytic activities of the as-prepared samples for degradation of methyl orange were carried in SGY-IB multi-purpose chemical reactor from Nanjing Hoop Technologies Co., Ltd., the light source was mercury lamp (300W, 225nm), and the system temperature was kept at 25±1°C using flowing cool water to remove the heat generated by mercury lamp. The electrospun fiber composites (0.29g containing 0.15g PbS-ZnS) were added in an aqueous solution(250mL) containing 0.005 g of methyl orange, while the PbS-ZnS powers(0.15g) and the P25-TiO_2 powders were dispersed in the same solution with a magnetic stirrer separately. The system was initially purged by N_2 in a dark environment to exclude the oxygen. The concentration of methyl orange was measured by UV/VIS spectrophotometer after photocatalytic degradation.

2.5. Characterization·

Scanning electron microscopy was carried out with a JSM-6490LV, which was bought from JEOL Co., Ltd. The X-ray diffraction (XRD)(Rigaku D/max-β B, Rigaku Corporation, Japan) measurement was carried out using a Cu-Kα radiation source. X-ray photoelectron spectroscopy (XPS) spectra was detected by the ESCALAB-MK-II. Ultraviolet-visible (UV-Vis) absorption spectra were obtained on a Shimadzu Solidepec-3700 DUV spectrophotometer at room temperature. The thermo-gravimetic analysis (TGA) was applied to evaluate the content of ZnS-PbS of PbS-ZnS/electrospun fiber composites on a Netzsch TG-209-F3. The high-voltage electrostatic generator was bought from Jinan Loufang Co., Ltd.

3. Results and discussion

3.1. Structure and morphology of composites

The SEM images of ZnS/ electrospun fiber composites, PbS-ZnS /electrospun fiber composites were shown in Fig. 1(a) and Fig. 1(b) respectively. The spherical ZnS particles with the diameter of about 600nm grew on the surface of the fibers. Fig. 1(b) showed that many PbS-ZnS particles grew on the surface of electrospun fibers. ZnS/electrospun fiber composites which were immersed in thiourea solution, there are numerous ZnS particles after reacting with thiourea. The size of PbS particles on the surface is to the point, and the particles distributed evenly.

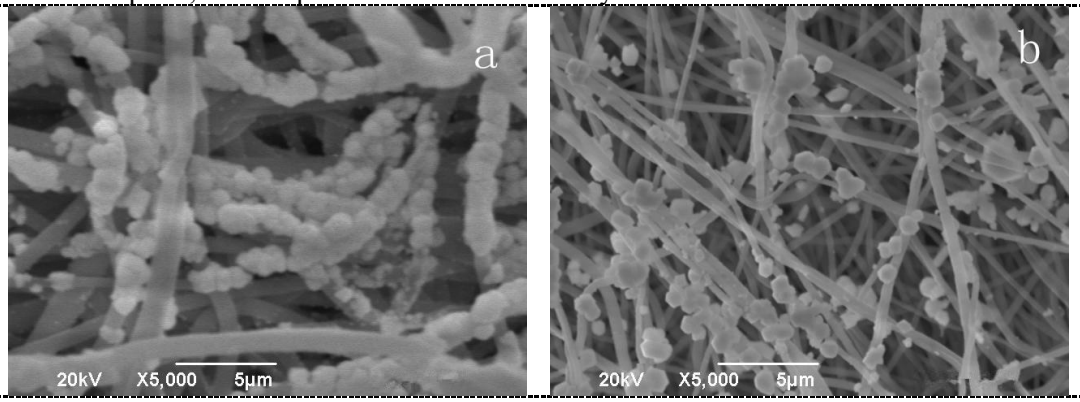

Figure 1. SEM images of (a) ZnS/ electrospun fiber composites, (b) PbS-ZnS /electrospun fiber composites.

Fig.2 showed the XRD patterns of ZnS/PVDF electrospun fiber composites and PbS-ZnS/PVDF electrospun fiber composites. The diffraction peaks located at 2θ = 28.47 °, 47.58 °, 56.22 °corresponded to the (111), (220) and (311) planes of the sphalerite structure of ZnS (ICDDPDF NO.05—0566). The diffraction peak appearing in Fig. 2(b) corresponded to the (111), (200), (220), (311), (222), and (440) planes of the galena crystal structure of PbS (JCPDS 5-0592), the narrow and sharp peaks indicate that the resulting product had a good crystalline state. The absorption peaks of ZnS and PVDF/SMA electrospun fibers were also shown in Fig. 2(b), which indicated that PbS-ZnS/electrospun fiber composites had been formed on the electrospun fibers.

XPS spectra of PbS-ZnS/electrospun fiber composites was showed in Fig.3. The spectra demonstrated that PbS-ZnS/electrospun fiber composites were composed of C, O, F, Zn, Pb and S elements, which were corresponding to the composites.

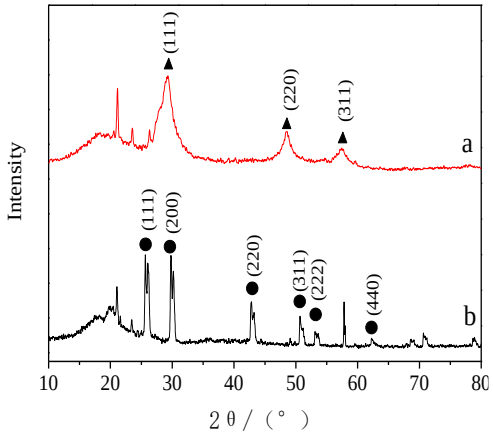

Figure 2. XRD patterns of (a) ZnS/ electrospun fiber composites (b)PbS-ZnS/ electrospun fiber composites

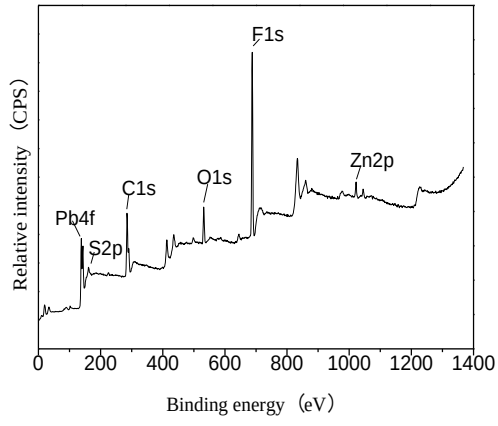

Figure 3. XPS spectra of PbS-ZnS/ electrospun fiber composites

3.2. Ultraviolet-Visible absorption spectra

Fig. 4.5 (a) shows the absorption of PbS-ZnS heterojunction/electrospun fiber composites at 350nm

had a maximum absorption peak, indicating that the photocatalyst can absorb ultraviolet light with a wavelength less than 360nm, which corresponded to the band gap value of sphalerite ZnS-PbS. In Fig. 4.5 (b), the unsupported electrospun fibers have no evident absorption between 300 and 800 nm, while composites have absorption peak sat round 280 nm, revealing that the conducting electrospun fibers do not interfere with the light absorption during the photocatalytic reaction.
Fig.5. shows the TGA curve of PbS-ZnS / electrospun fiber composites. The final mass loss of PVDF / SMA electrospun fibers is 93% by TGA, while the final weight loss of PbS-ZnS heterojunction/ electrospun fiber composites after loading is 45.23%, so the mass fraction of catalyst is about 51.36%.

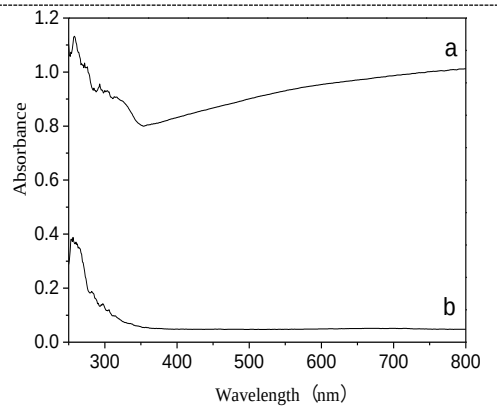

Figure 4. UV/VIS absorption spectra of (a) PbS-ZnS/ electrospun fiber composites (b) PVDF/SMA electrospun fiber

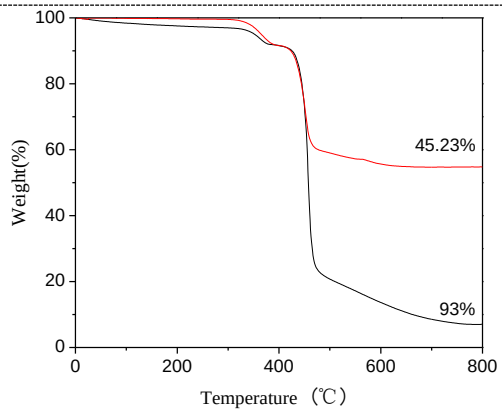

Figure 5. TGA curve of PbS-ZnS/ electrospun fiber composites

3.3. Photocatalytic activity measurements
The photocatalytic performance of PbS-ZnS / electrospun fiber composites was evaluated by degradation of methyl orange under ultraviolet (UV) light irradiation of solar light. The degree of the photocatalysis is presented by the ratio of the concentration C/C_0 under various times. Fig.6 shows the trend of photocatalytic degradation. It can be clearly observed that the residual mass fraction of methyl orange was 1.23% after PbS-ZnS/electrospinning fiber composites photo-degradation for 300 min, while the removal efficiency of methyl orange reaches to 32.4% by PbS-ZnS powders and 44.2% by P25-TiO_2 powders. This shows that the photocatalytic degradation of PbS-ZnS/electrospinning fiber composite is much more efficient than PbS-ZnS heterojunction powders and P25-TiO_2 powders, which is due to the the PbS-ZnS heterojunction loaded on the surface of the electrospun fiber have a larger surface area and higher light utilization. In addition, the PVDF/SMA electrospinning fiber has strong adsorption capacity, which makes it easy for methyl orange to be absorbed and migrated to the surface of inorganic particles of composite materials, performs photocatalytic degradation of methyl orange and forms an adsorption-migration-photo degradation chain. However, the adsorption capacity of PbS-ZnS heterojunction powders is so weak that the process of the entry of -OH reactive groups into the solution becomes the key factor of photodegradation rate. In addition, as can be seen from Fig. 6, the degradation rate of PbS-ZnS heterojunction powders is significantly higher than that of Degussa P25-TiO_2, which is due to the special band structure and carrier transport characteristics of semiconductor heterojunctions.

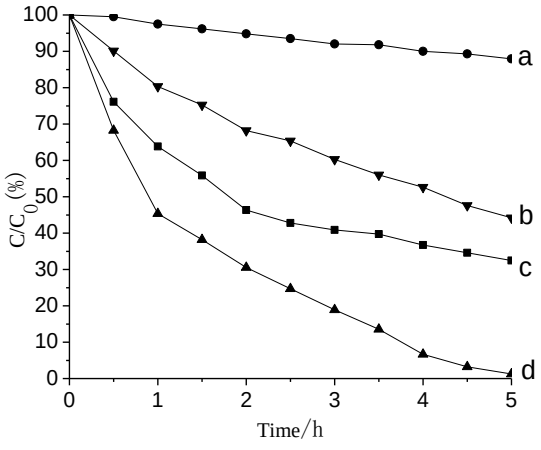

Figure 6. Photocatalytic degradation by (a) PVDF/SMA electrospun fiber (b) Degussa P25 TiO2 (c) The PbS-ZnS powder (d) The PbS-ZnS / electrospunning fiber composite

There are three possible reasons for this phenomenon (Fig.7). Firstly, when PbS-ZnS heterojunction particals were loaded on the surface of the fibers, they have a large specific surface area and high-energy efficiency of UV irradiation. Secondly, the carrier can prevent the loss and degradation of the powdery catalyst. Thirdly, the photo-generated eletron-hole pairs within the PbS-ZnS heterojunction particles were produced in the light, the electron migrate to the surface of the PbS and degraded methyl orange in water. The holes which migrate to the surface of the electrospun fiber and react with the sacrificial agents were adsorbed on the surface of the fiber.

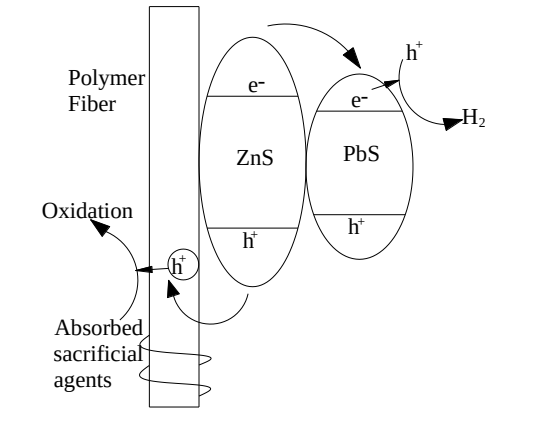

Figure7. Structure and catalytic mechanism diagram of PbS-ZnS/electrospun fiber composites

4. Conclusion

In summary, novel composite photocatalysts- PbS-ZnS/electrospun fiber composites were successfully synthesized and had an obvious effect on enhancing the photocatalytic efficiency of the photocatalysts. The UV-Vis absorption spectra of PbS-ZnS / electrospun fiber composites shows that the materials have good absorption under visible light, and electrospun fiber absorption peak in the mercury lamp simulated sunlight catalytic hydrogen water does not affect the light absorption of the composite. The residual mass fraction of methyl orange was 1.23% after PbS-ZnS/electrospinning fiber composites photo-degradation for 300 min, which is better than PbS-ZnS heterojunction powders and P25-TiO_2 powders.

Acknowledgements

This work is supported by the Natural Science Foundation of Jiangsu Educational committee (No. 18KJD480001) and No. YZGXYJS2018-KYCX-012.

References

[1].Fujishima, A.; Honda, K., 1972, Electrochemical photolysis of water at a semiconductor electrode. *Nature* 238, (5358), 37-8.
[2].Gaya, U. I.; Abdullah, A. H., 2008, Heterogeneous photocatalytic degradation of organic contaminants over titanium dioxide: A review of fundamentals, progress and problems. *Journal of Photochemistry and Photobiology C-Photochemistry Reviews* 9, (1), 1-12.
[3].Li, Z.; Qiu, N.; Yang, G., 2009, Effects of synthesis parameters on the microstructure and phase structure of porous 316L stainless steel supported TiO2 membranes. *J. Membr. Sci.* 326, (2), 533-538.
[4].Du, M.; Du, Y.; Feng, Y.; Yang, K.; Lv, X.; Jiang, N.; Liu, Y., 2018, Facile preparation of BiOBr/cellulose composites by in situ synthesis and its enhanced photocatalytic activity under visible-light. *Carbohydr. Polym.* 195, 393-400.
[5].Fan, W.-J.; Zhou, Z.-F.; Xu, W.-B.; Shi, Z.-F.; Ren, F.-M.; Ma, H.-H.; Huang, S.-W., 2010, Preparation of ZnIn(2)S(4)/fluoropolymer fiber composites and its photocatalytic H(2) evolution from splitting of water using Xe lamp irradiation. *Int. J. Hydrogen Energy* 35, (13), 6525-6530.
[6].He, T.; Zhou, Z.; Xu, W.; Ren, F.; Ma, H.; Wang, J., 2009, Preparation and photocatalysis of TiO2-fluoropolymer electrospun fiber nanocomposites. *Poly* 50, (13), 3031-3036.
[7].Grilla, E.; Petala, A.; Frontistis, Z.; Konstantinou, I. K.; Kondarides, D. I.; Mantzavinos, D., 2018, Solar photocatalytic abatement of sulfamethoxazole over Ag3PO4/WO3 composites. *Applied Catalysis B-Environmental* 231, 73-81.
[8].Zheng, J.; Zhang, L., 2018, Rational design and fabrication of multifunctional catalyzer CO2SnO4-SnO2/GC for catalysis applications: Photocatalytic degradation/catalytic reduction of organic pollutants. *Applied Catalysis B-Environmental* 231, 34-42.
[9].Zhou, X.; Shi, T.; Zhou, H., 2012, Hydrothermal preparation of ZnO-reduced graphene oxide hybrid with high performance in photocatalytic degradation. *Appl. Surf. Sci.* 258, (17), 6204-6211.
[10].Pelaez, M.; Nolan, N. T.; Pillai, S. C.; Seery, M. K.; Falaras, P.; Kontos, A. G.; Dunlop, P. S. M.; Hamilton, J. W. J.; Byrne, J. A.; O'Shea, K.; Entezari, M. H.; Dionysiou, D. D., 2012, A review on the visible light active titanium dioxide photocatalysts for environmental applications. *Applied Catalysis B-Environmental* 125, 331-349.
[11].Tong, H.; Ouyang, S.; Bi, Y.; Umezawa, N.; Oshikiri, M.; Ye, J., 2012, Nano-photocatalytic Materials: Possibilities and Challenges. *Adv. Mater.* 24, (2), 229-251.
[12].Guo, X.; Zhou, X.; Li, X.; Shao, C.; Han, C.; Li, X.; Liu, Y., 2018, Bismuth oxychloride (BiOCl)/copper phthalocyanine (CuTNPc) heterostructures immobilized on electrospun polyacrylonitrile nanofibers with enhanced activity for floating photocatalysis. *J. Colloid Interface Sci.* 525, 187-195.
[13].Konstantinou, I. K.; Albanis, T. A., 2004, TiO2-assisted photocatalytic degradation of azo dyes in aqueous solution: kinetic and mechanistic investigations - A review. *Applied Catalysis B-Environmental* 49, (1), 1-14.